

# Twisting Carbon Nanotube Fibers for Both Wire-Shaped Micro-Supercapacitor and Micro-Battery

Jing Ren, Li Li, Chen Chen, Xuli Chen, Zhenbo Cai, Longbin Qiu, Yonggang Wang,\*  
Xingrong Zhu, and Huisheng Peng\*

Energy storage systems including supercapacitors and lithium ion batteries typically appear in a rigid plate which is unfavorable for many applications, especially in the fields of portable and highly integrated equipments which require small size, light weight, and high flexibility.<sup>[1–3]</sup> As a result, flexible supercapacitors and batteries mainly in a film format have been widely investigated, while wire-shaped energy storage devices are rare.<sup>[4,5]</sup> However, compared with the conventional planar structure, a wire device can be easily woven into textiles or other structures to exhibit unique and promising applications. The limitation is originated from the much stricter requirement for the electrode such as a combined high flexibility and electrochemical property in wire-shaped devices.<sup>[6,7]</sup> It remains challenging but becomes highly desired to obtain wire-shaped supercapacitors and batteries with high performances.

On the other hand, due to the unique structure and remarkable mechanical and electrical properties, carbon nanotubes (CNTs) have been widely studied as electrode materials in conventional planar energy storage devices.<sup>[8,9]</sup> However, CNTs are generally made in a network format in which the produced charges had to cross a lot of boundaries with low efficiencies. It is critically important to improve the charge transport in CNT materials.<sup>[8–13]</sup>

Herein, we have developed wire-shaped micro-supercapacitors and micro-batteries with high performances by using aligned multi-walled carbon nanotube (MWCNT) fibers as electrodes. The micro-supercapacitor wire was fabricated by twisting

two aligned MWCNT fibers and showed a mass specific capacitance of 13.31 F/g, area specific capacitance of 3.01 mF/cm<sup>2</sup>, or length specific capacitance of 0.015 mF/cm at  $2 \times 10^{-3}$  mA (1.67 A/g). The wire-shaped battery was produced by twisting an aligned MWCNT fiber and a lithium wire which functioned as positive and negative electrodes, respectively. The specific capacity was calculated as 94.37 mAh/cm<sup>3</sup> or 174.40 mAh/g at  $2 \times 10^{-3}$  mA. The energy and power densities in both supercapacitors and batteries could be further greatly improved by incorporation of MnO<sub>2</sub> nanoparticles into MWCNT fibers. For instance, the charge and discharge energy densities achieved 92.84 and 35.74 mWh/cm<sup>3</sup> while the charge and discharge power densities were 3.87 and 2.43 W/cm<sup>3</sup> at  $2 \times 10^{-3}$  mA in the wire-shaped micro-battery.

Spinnable MWCNT arrays were first synthesized by chemical vapor deposition, and aligned MWCNT fibers could then be spun from the array with controlled diameters from 2 to 30  $\mu$ m and lengths up to 100 m. Figure S1a shows a typical scanning electron microscopy (SEM) image of MWCNT fiber with uniform diameter of 20  $\mu$ m. Figure 1a further shows that MWCNTs are highly aligned in the fiber, which enables high tensile strengths up to 1.3 GPa and high electrical conductivities of 10<sup>3</sup> S/cm. Therefore, the MWCNT fibers had been further used as electrodes to deposit MnO<sub>2</sub> on the MWCNTs to produce composite fibers, and the content of MnO<sub>2</sub> was controlled

J. Ren,<sup>[†]</sup> L. Li, C. Chen, X. Chen, Z. Cai, L. Qiu, X. Zhu,

Prof. H. Peng

State Key Laboratory of Molecular

Engineering of Polymers

Department of Macromolecular Science

and Laboratory of Advanced Materials

Fudan University, Shanghai 200438, China

E-mail: penghs@fudan.edu.cn

Dr. L. Li<sup>[†]</sup>

College of Food Science and Technology

Shanghai Ocean University

Shanghai 201306, China

Prof. Y. Wang

Department of Chemistry and Shanghai Key Laboratory of Molecular

Catalysis and Innovative Materials

Institute of New Energy

Fudan University

Shanghai 200438, China

E-mail: ygwang@fudan.edu.cn

[†] These authors contributed equally to this work.

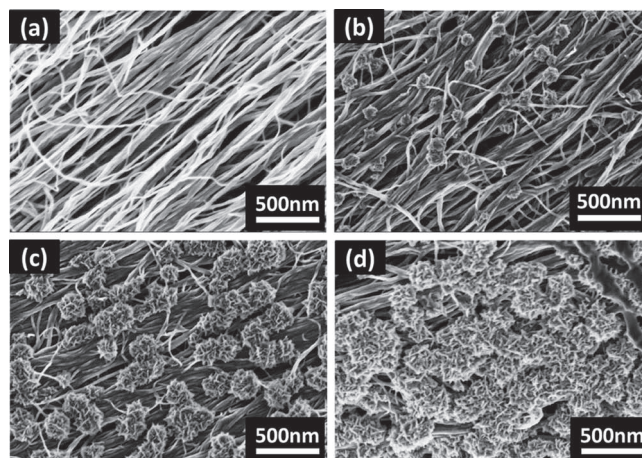


**Figure 1.** Scanning electron microscopy (SEM) images of aligned MWCNT fibers before and after electrodeposition of MnO<sub>2</sub> nanoparticles. a) Bare fiber. b) Composite fiber with MnO<sub>2</sub> weight percentage of 0.5%. c) Composite fiber with MnO<sub>2</sub> weight percentage of 4.1%. d) Composite fiber with MnO<sub>2</sub> weight percentage of 8.6%.

DOI: 10.1002/adma.201203445

by the cycle number of electrodeposition.<sup>[14,15]</sup> Figures S1b-S1d and 1b-1d show SEM images of representative MWCNT/MnO<sub>2</sub> composite fibers with the increasing weight percentages of MnO<sub>2</sub> from 0.5 to 8.6%. MnO<sub>2</sub> was uniformly deposited on MWCNTs in a format of nanoparticles, and their diameters were increased with the increasing MnO<sub>2</sub> weight percentage, e.g., 110, 240, and 340 nm at 0.5, 4.1, and 8.6%, respectively. After the electrodeposition of MnO<sub>2</sub> nanoparticles, the high flexibility, strengths and conductivities in the fiber had been all well maintained.

Raman spectroscopy further showed that the intensity ratio of D to G band in the composite fiber was maintained to be 1.15 after bending for over one hundred cycles, indicating a stable attachment of MnO<sub>2</sub> nanoparticles on MWCNTs.<sup>[16]</sup> A typical Raman spectrum is shown in Figure S2. In fact, no obvious decrease in structure integrity had been traced by SEM either. As a result, the excellent properties of composite fibers could be also well maintained during the deformation. For instance, the electrical resistance remained almost unchanged during the bending process monitored by a multimeter.

Two bare MWCNT fibers or Two MWCNT/MnO<sub>2</sub> composite fibers were then used as parallel electrodes to produce wire-shaped micro-supercapacitors. The average specific capacitance of supercapacitor was calculated by the following equation:  $C = 2i_0/[m(\Delta V/\Delta t)]$ , where  $i_0$ ,  $\Delta V/\Delta t$  and  $m$  correspond to the discharge current, average slope of the discharge curve, and mass of the active material in the electrode, respectively. Figure 2a and 2b have compared the dependence of specific capacitances on current between  $5 \times 10^{-4}$  and  $1 \times 10^{-2}$  mA for the bare and composite fibers. The specific capacitances were reduced with the increasing current in both cases, i.e., from 3.53 to 3.01 mF/cm<sup>2</sup> (or 0.018 to 0.015 mF/cm) for the bare fiber and from 3.57 to 3.16 mF/cm<sup>2</sup> (or 0.019 to 0.016 mF/cm) for the composite fiber with MnO<sub>2</sub> weight percentage of 4.1%. However, the reduced degree for the composite fiber was much lower than the bare fiber. In order to compare with other systems, the mass specific capacitances could be also obtained such as 15.61 to 13.31 F/g with the increasing current of  $5 \times 10^{-4}$  to  $1 \times 10^{-2}$  mA for the bare fiber. This mass specific capacitance was about three times of the other reports.<sup>[17,18]</sup> The flexible solid-state micro-supercapacitor in an aqueous electrolyte of H<sub>3</sub>PO<sub>4</sub> and poly(vinyl alcohol)<sup>[19]</sup> had also been successfully fabricated, but the specific capacitance was relatively low in the voltage window of 0 – 1 V, e.g., 0.006 mF/cm for bare MWCNT fibers and 0.014 mF/cm for composite fibers at  $2 \times 10^{-3}$  mA. Note that the conventional planar supercapacitor based on the CNT/MnO<sub>2</sub> composite as electrodes showed a higher specific capacitance.<sup>[20,21]</sup> More efforts are underway to improve the performance of such wire-shaped device. Figure 2c has further shown that the area specific capacitances increase with the increasing MnO<sub>2</sub> content. It is reasonable considering that MnO<sub>2</sub> nanoparticles have contributed higher pseudo-capacitances than MWCNTs.<sup>[22,23]</sup>

The cyclic performances of supercapacitors derived from bare MWCNT and composite fibers were further investigated in 1000 cycles at a discharge current of  $2 \times 10^{-3}$  mA (Figure 3a and 3b). The specific capacitances were varied in less than 3% for both bare MWCNT and composite fibers. Cyclic voltammetry was also used to study the high stability of the supercapacitor wires. The inserted graphs in Figure 3a and 3b compare

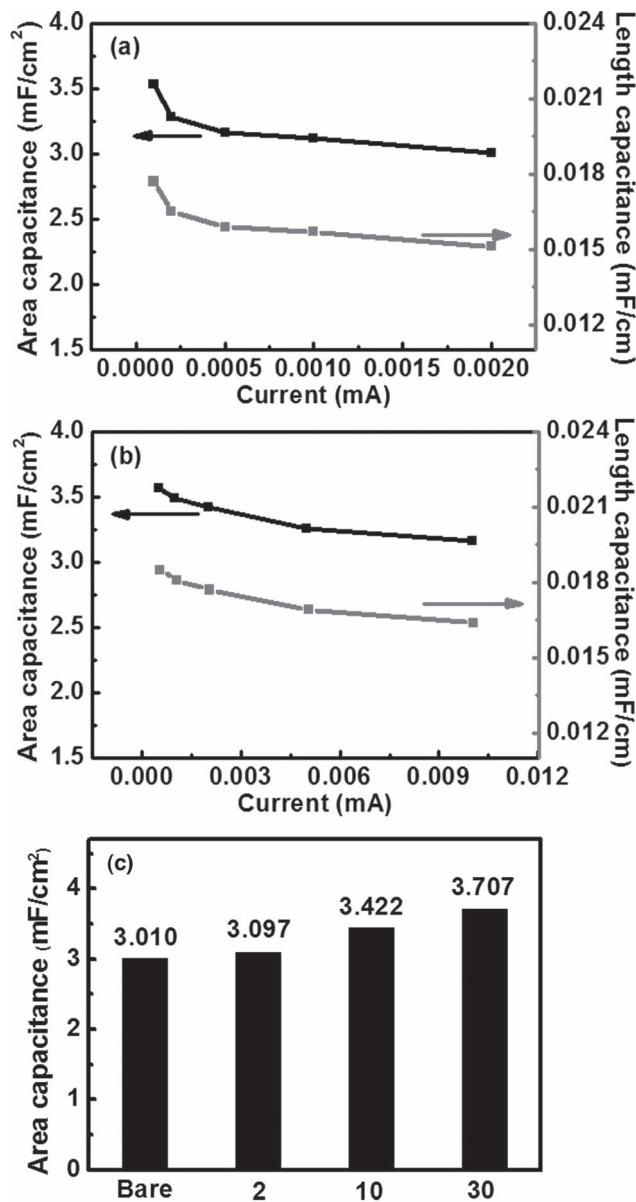


**Figure 2.** Dependence of specific capacitance in the supercapacitor wire on the current. a) Twisting two bare MWCNT fibers. b) Twisting two MWCNT/MnO<sub>2</sub> composite fibers. c) A comparison between bare and composite fibers with the increasing MnO<sub>2</sub> weight percentage at a current of  $2 \times 10^{-3}$  mA.

cyclic voltammograms (CVs) based on bare MWCNT fibers and MWCNT/MnO<sub>2</sub> composite fibers with MnO<sub>2</sub> weight percentage of 4.1% measured by a two-electrode system in LB303 electrolyte. The rectangular shape which corresponds to an electrochemical double layer capacitor had been well maintained at a high scan rate up to 10 V/s for the supercapacitor derived from bare MWCNT fibers. Pure MnO<sub>2</sub> nanoparticles showed a pseudo-capacitance, but different from conducting polymers such as polyaniline, the resulting supercapacitor exhibited rectangular CV curves without obvious peaks.<sup>[22,23]</sup> As a result, the supercapacitor wires based on composite fibers

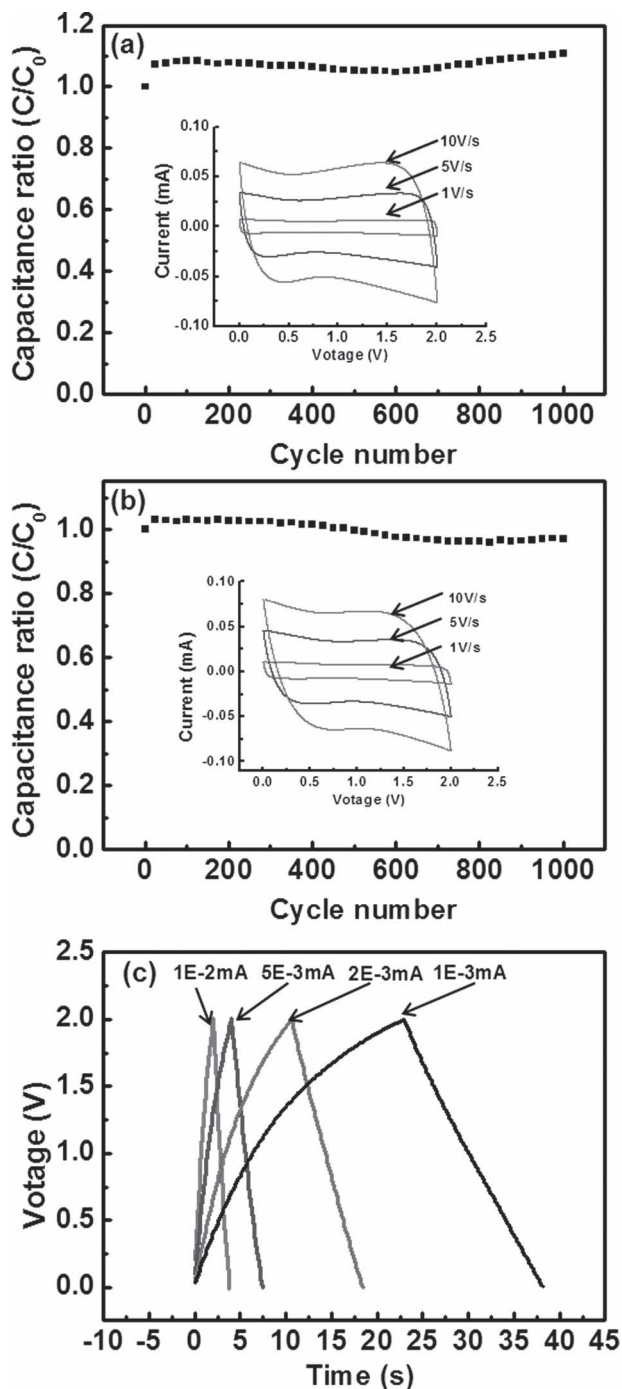


**Figure 3.** a) and b) Dependence of specific capacitance for supercapacitors by twisting two bare MWCNT fibers and two MWCNT/MnO<sub>2</sub> composite fibers on bent cycle number, respectively (inserted, CV curves at different scan rates).  $C_0$  and  $C$  correspond to the specific capacitance at the first and following cycle, respectively. c) Galvanostatic charge/discharge curves for a supercapacitor wire by twisting two MWCNT/MnO<sub>2</sub> composite fibers with the MnO<sub>2</sub> weight percentage of 8.6%.

produced rectangular shapes which had also been well maintained at high scan rates such as 10 V/s. Figure 3c further compares charge-discharge curves of the supercapacitor based on composite fibers under different current densities. The time

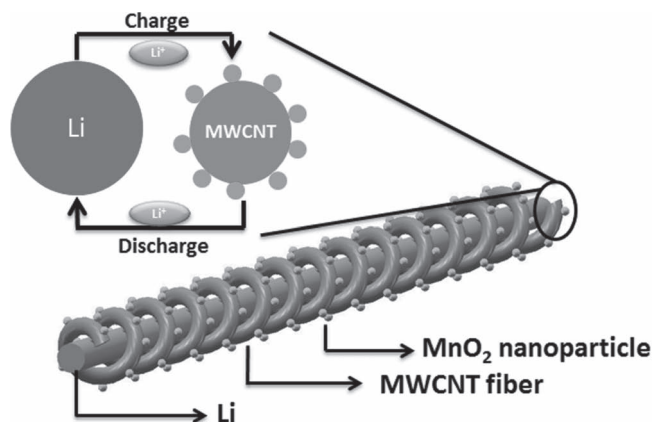


**Figure 4.** Schematic illustration to the wire-shaped lithium ion battery fabricated by twisting an aligned MWCNT/MnO<sub>2</sub> composite fiber and Li wire as positive and negative electrodes, respectively. The inserted top left image shows the charge-discharge process.

duration was increased with the decreasing current from  $1 \times 10^{-2}$  to  $1 \times 10^{-3}$  mA. Nevertheless, the charge-discharge curves were similar in shape between 2 and 0 V, indicating that the composite fiber-based supercapacitor could be stably performed in a wide range of currents.

Either bare or composite fiber had been further twisted with a Li wire to produce wire-shaped lithium ion batteries. Figure 4 schematically shows the battery structure with the bare or composite fiber as positive electrode and Li wire as negative electrode. The specific capacity of battery was calculated from the discharge profiles by equation of  $C_1 = (I \times \Delta t)/m$  or  $C_2 = (I \times \Delta t)/V$ , where  $C_1$ ,  $C_2$ ,  $I$ ,  $\Delta t$ ,  $m$ , and  $V$  correspond to mass specific capacity (mAh/g), volumetric specific capacity (mAh/cm<sup>3</sup>), applied current (mA), discharge time (s), mass (g) and geometric volume (cm<sup>3</sup>) of active fiber, respectively. Figure 5a shows typical charge and discharge curves of the battery wire based on a bare MWCNT fiber at  $5 \times 10^{-4}$  mA. Obviously, the resulting battery showed a very low operating voltage ( $\sim 0.4$  V) as MWCNTs exhibited very low Li<sup>+</sup> intercalation/deintercalation potential and were generally considered as negative materials for conventional lithium-ion batteries, not positive materials.<sup>[24,25]</sup> To this end, the aligned MWCNT/MnO<sub>2</sub> composite fiber may serve as a good candidate for a positive electrode. In fact, a discharge platform to about 1.5 V had been found for the battery based on the composite fiber (Figure 5b). The battery had achieved a specific capacity of 109.62 mAh/cm<sup>3</sup> (or 218.32 mAh/g) at a current of  $5 \times 10^{-4}$  mA. Figure 5c further shows that the specific capacity decreases with the increasing current. When the applied current was increased to  $5 \times 10^{-3}$  mA, the battery derived from the composite fiber showed a lower specific capacity of 8.45 mAh/cm<sup>3</sup>. Obviously, the capacity retention of micro-battery with the increasing current was much lower than the micro-supercapacitor mainly due to their different energy storage mechanisms. For supercapacitors, the capacitance mainly arises from the surface reaction of electrode materials, including surface charge separations at electrode/electrolyte interfaces and surface faradic redox reactions which are not controlled by the ion diffusion process.<sup>[23]</sup> For batteries, the capacity mainly relies

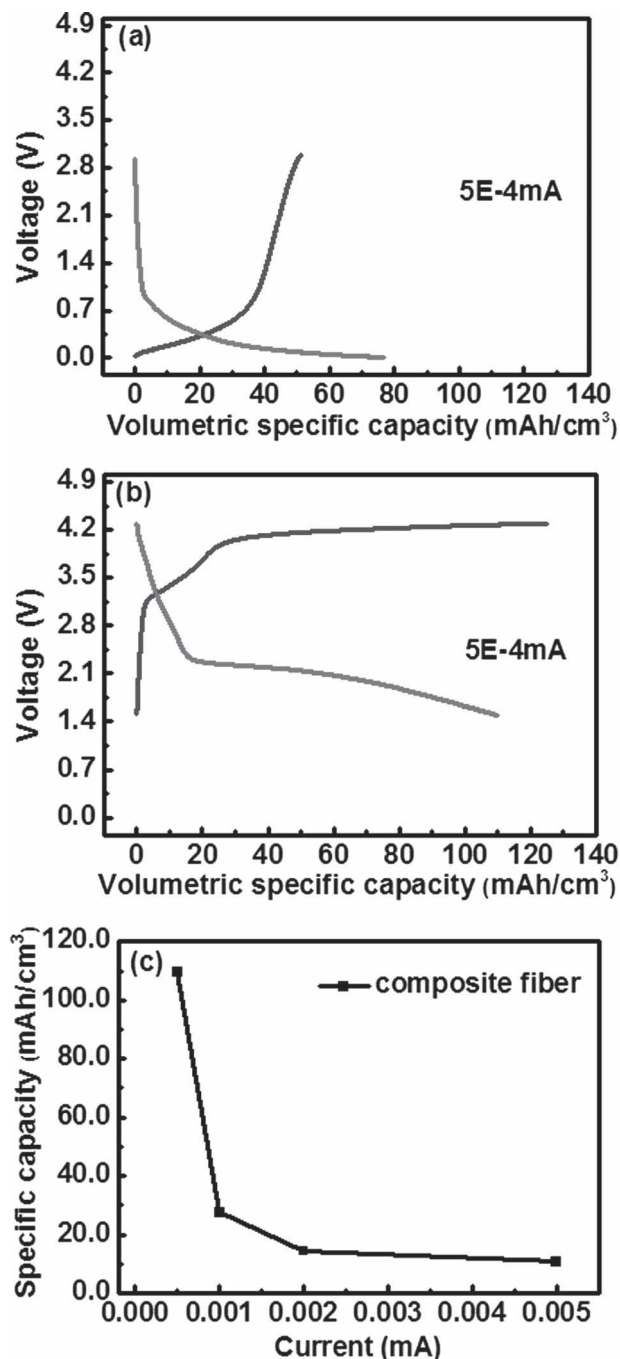


**Figure 5.** Charge and discharge of wire-shaped batteries at a current of  $5 \times 10^{-4}$  mA. a) A bare MWCNT fiber and Li as electrodes. b) An MWCNT/MnO<sub>2</sub> composite fiber with the MnO<sub>2</sub> weight percentage of 4.1% and Li as electrodes. c) Dependence of specific capacitance for a battery wire derived from the MWCNT/MnO<sub>2</sub> composite fiber with MnO<sub>2</sub> weight percentage of 4.1% on current.

on faradic redox reactions in the crystalline framework of electrode materials which require long-range ion diffusions. When tested at a higher current, the batteries showed lower capacities derived from a slower ion diffusion rate in the crystalline framework of electrode materials.

**Table 1.** The energy density and power density of wire-shaped micro-supercapacitors and micro-batteries derived from MWCNT/MnO<sub>2</sub> composite fibers with MnO<sub>2</sub> weight percentage of 4.1% at a current of  $2 \times 10^{-3}$  mA.

Process	Supercapacitor		Lithium ion battery	
	mWh/cm <sup>3</sup>	W/cm <sup>3</sup>	mWh/cm <sup>3</sup>	W/cm <sup>3</sup>
Charge	3.47	1.08	92.84	3.87
Discharge	1.73	0.79	35.74	2.43

Table 1 has further compared the highest energy density and power density of wire-shaped micro-supercapacitors and micro-batteries based on the aligned MWCNT/MnO<sub>2</sub> composite fibers. From supercapacitor to battery, the energy densities were greatly improved for about 26 and 20 times, and the power densities had been also enhanced by 258 and 208% during the charge and discharge process, respectively. The improved energy and power densities are explained by the fact that the charge storage occurs not only on the surface but also within the crystalline framework of electrode materials in battery, while the charge storage only takes place on the surface of electrode materials in supercapacitor. Currently, the energy densities achieved 92.84 and 35.74 mWh/cm<sup>3</sup> while the power densities could reach 3.87 and 2.43 W/cm<sup>3</sup> during the charge and discharge process in battery, respectively.

In summary, aligned MWCNT fibers and composite fibers have been easily twisted to produce both wire-shaped supercapacitors and lithium ion batteries with high capacitive performances. The combined flexible wire structure and high tensile strength also enable promising applications in various fields, e.g., these wires can be easily integrated into electronic textiles by a conventional weaving technique. This work further presents a fabrication paradigm in the development of novel storage devices by using strong and conductive nanostructured fibers as effective electrodes.

## Experimental Section

The synthesis of MWCNT arrays and preparation of aligned MWCNT fibers were made according to the literature.<sup>[6,7,26,27]</sup> The MnO<sub>2</sub> nanoparticles were electrochemically deposited on MWCNT fibers in an aqueous solution including 0.05M Mn(CH<sub>3</sub>COO)<sub>2</sub> and 0.10M Na<sub>2</sub>SO<sub>4</sub> at a potential range of -0.2 to 0.8 V (vs. Ag/AgCl) through an electrochemical analyzer system (CHI 660D). The structures were characterized by scanning electron microscopy (SEM, Hitachi FE-SEM S-4800 operated at 1 kV) and Raman spectroscopy (Dilor LabRam-1B, He-Ne laser of 4 mW, excitation wavelength of 632.8 nm). For two bare MWCNT or MWCNT/MnO<sub>2</sub> composite fibers, one end of each fiber was firstly fixed and connected to a copper wire by silver paint. To produce a supercapacitor wire, two fibers could be arranged in a parallel format without the use of a separator or twisted by using the conventional polyvinylidene fluoride as the separator. Here one fiber functioned as the working electrode with the other as both counter and reference electrode. In the case of a battery, one bare or composite fiber was replaced with a Li wire. For both supercapacitor and battery, LiPF<sub>6</sub> in a mixture solvent of ethylene carbonate, diethyl carbonate and dimethyl carbonate (weight ratios of 1/1/1) with a concentration of 1 M (also called LB303) was used as the non-aqueous electrode. In the case of solid-state micro-supercapacitors in an aqueous electrolyte, a mixture of H<sub>3</sub>PO<sub>4</sub> and poly (vinyl alcohol)

with a weight ratio of 1/1 was used. The cyclic voltammetry was made by a CHI 660C electrochemical workstation at room temperature with a scan rate range of 0.01 to 10 V/s by a three-electrode method. Galvanostatic charge/discharge measurements were made at a current range of  $5 \times 10^{-4}$  to  $1 \times 10^{-2}$  mA by an ARBIN electrochemical workstation (MSTAT-5 V/10 mA/16Ch). The potential ranges were measured from 0 to 2 V for supercapacitors, 0.05 to 3 V for the batteries based on bare MWCNT fibers and 1.5 to 4.3 V for the batteries based on MWCNT/MnO<sub>2</sub> composite fibers.

## Supporting Information

Supporting Information is available from the Wiley Online Library or from the author.

## Acknowledgements

This work was supported by NSFC (20904006, 91027025), MOST (2011CB932503, 2011DFA51330), MOE (NCET-09-0318), STCSM (11520701400), CPSF (2011M500724), The Program for Professor of Special Appointment (Eastern Scholar) at Shanghai Institutions of Higher Learning and State Key Laboratory of Molecular Engineering of Polymers at Fudan University (K2011-10).

Received: August 20, 2012

Revised: October 4, 2012

Published online: November 22, 2012

- 
- [1] X. B. Yan, Z. X. Tai, J. T. Chen, Q. J. Xue, *Nanoscale* **2011**, *3*, 212.  
[2] A. G. Pandolfo, A. F. Hollenkamp, *J. Power Sources* **2006**, *157*, 11.  
[3] H.-X. Zhang, C. Feng, Y.-C. Zhai, K.-L. Jiang, Q.-Q. Li, S.-S. Fan, *Adv. Mater.* **2009**, *21*, 2299.  
[4] S.-L. Chou, J.-Z. Wang, S.-Y. Chew, H.-K. Liu, S.-X. Dou, *Electrochem. Commun.* **2008**, *10*, 1724.  
[5] L. Hu, H. Wu, F. La Mantia, Y. Yang, Y. Cui, *ACS Nano* **2010**, *4*, 5843.  
[6] T. Chen, L. Qiu, Z. Cai, F. Gong, Z. Yang, Z. Wang, H. Peng, *Nano Lett.* **2012**, *12*, 2568.  
[7] T. Chen, L. Qiu, H. G. Kia, Z. Yang, H. Peng, *Adv. Mater.* **2012**, *24*, 4623.  
[8] K. Jiang, J. Wang, Q. Li, L. Liu, C. Liu, S. Fan, *Adv. Mater.* **2011**, *23*, 1154.  
[9] K. Liu, Y. Sun, R. Zhou, H. Zhu, J. Wang, L. Liu, S. Fan, K. Jiang, *Nanotechnology* **2010**, *21*, 045708.  
[10] H. Peng, M. Jain, D. E. Peterson, Y. Zhu, Q. Jia, *Small* **2008**, *4*, 1964.  
[11] F. Deng, W. Lu, H. Zhao, Y. Zhu, B.-S. Kim, T.-W. Chou, *Carbon* **2011**, *49*, 1752.  
[12] Z. Yang, X. Sun, X. Chen, Z. Yong, G. Xu, R. He, Z. An, Q. Li, H. Peng, *J. Mater. Chem.* **2011**, *21*, 13772.  
[13] X. Zhang, Q. Li, Y. Tu, Y. Li, J. Y. Coulter, L. Zheng, Y. Zhao, Q. Jia, D. E. Peterson, Y. Zhu, *Small* **2007**, *3*, 244.  
[14] Z. Fan, J. Chen, M. Wang, K. Cui, H. Zhou, Y. Kuang, *Diamond Rel. Mater.* **2006**, *15*, 1478.  
[15] J. M. Ko, K. M. Kim, *Mater. Chem. Phys.* **2009**, *114*, 837.  
[16] W. Guo, C. Liu, X. Sun, Z. Yang, H. G. Kia, H. Peng, *J. Mater. Chem.* **2012**, *22*, 903.  
[17] A. B. Dalton, S. Collins, E. Munoz, J. M. Razal, V. H. Ebron, J. P. Ferraris, J. N. Coleman, B. G. Kim, R. H. Baughman, *Nature* **2003**, *423*, 703.  
[18] J. Bae, M. K. Song, Y. J. Park, J. M. Kim, M. Liu, Z. L. Wang, *Angew. Chem. Int. Ed.* **2011**, *50*, 1683.  
[19] M. Q. Xue, Z. Xie, L. S. Zhang, X. L. Ma, X. L. Wu, Y. G. Guo, W. G. Song, Z. B. Li, T. B. Cao, *Nanoscale* **2011**, *3*, 2703.  
[20] L. Hu, W. Chen, X. Xie, N. Liu, Y. Yang, H. Wu, Y. Yao, M. Pasta, H. N. Alshareef, Y. Cui, *ACS Nano* **2011**, *5*, 8904.  
[21] Y. Hou, Y. W. Cheng, T. Hobson, J. Liu, *Nano Lett.* **2010**, *10*, 2727.  
[22] a) M. Toupin, T. Brousse, D. Bélanger, *Chem. Mater.* **2004**, *16*, 3184; b) J. X. Zhu, W. H. Shi, N. Xiao, X. H. Rui, H. T. Tan, X. H. Lu, H. H. Hng, J. Ma, Q. Y. Yan, *ACS Appl. Mater. Interfaces* **2012**, *4*, 2769.  
[23] P. Simon, Y. Gogotsi, *Nat. Mater.* **2008**, *7*, 845.  
[24] B. J. Landi, M. J. Ganter, C. D. Cress, R. A. DiLeo, R. P. Raffaele, *Energy Environ. Sci.* **2009**, *2*, 638.  
[25] J. Chen, A. I. Minett, Y. Liu, C. Lynam, P. Sherrell, C. Wang, G. G. Wallace, *Adv. Mater.* **2008**, *20*, 566.  
[26] Z. Yang, T. Chen, R. He, G. Guan, H. Li, L. Qiu, H. Peng, *Adv. Mater.* **2011**, *23*, 5436.  
[27] L. Li, Z. Yang, H. Gao, H. Zhang, J. Ren, X. Sun, T. Chen, H. G. Kia, H. Peng, *Adv. Mater.* **2011**, *23*, 3730.